Counterion Condensation in Solutions of Rigid Polyelectrolytes

Rebecca M. Nyquist, Bae-Yeun Ha, and Andrea J. Liu

Department of Chemistry and Biochemistry, UCLA, Los Angeles, California 90095

Received July 14, 1998; Revised Manuscript Received November 13, 1998

ABSTRACT: We present a simple theory to examine counterion condensation in isotropic solutions of finite-length rigid polyelectrolytes. Electrostatic interactions are described by an extension of Debye−Hückel theory, in which a wavevector-dependent screening length takes into account the connectivity of the polyions. The counterions are divided into two classes, free and condensed, in chemical equilibrium. We demonstrate that trends in counterion condensation are affected by the polyion concentration, the polyion shape, and the solvent quality and that these trends in counterion condensation in turn affect the phase behavior and osmotic pressure of the polyelectrolyte solution.

1. Introduction

Polyelectrolytes are polymers with ionizable groups that dissociate in polar solvent into charges bound to the chain and counterions in solution. Many properties of the resulting solution, such as conductivity and osmotic pressure, depend sensitively on the spatial distribution of the counterions. Entropy of mixing drives the counterions to distribute uniformly, whereas electrostatic interactions attract the counterions to the oppositely charged polymer chains. For a single, infinitely long, rigid rod at zero concentration, the counterion distribution around the rod can be calculated using the Poisson−Boltzmann (PB) equation.[1−3] An alternate, two-state model developed by Manning[4] and Oosawa,[5] however, simplifies the problem further by replacing the spatial distribution of counterions with a step function. Counterions are thus divided into two species: *free*, those that have been driven to infinity by entropy of mixing, and *condensed*, those whose entropy of mixing has been overcome by electrostatic attraction to the rod and are found within some finite distance of the rod. The competition between the logarithmic electrostatic attraction of the counterions to the rod and the logarithmic entropic gain driving counterions away from the rod results in a nonzero fraction of condensed counterions for sufficiently strongly charged rods. This phenomenon is known as counterion condensation. The condensed counterions partially neutralize the bare-rod charge density uniformly to a *net* charge density. This quantity is important to the interpretation of experiments on polyelectrolyte solutions and is often assumed to be given by the Manning/Oosawa (MO) theory.[6−9] However, MO theory applies to an infinite line charge at zero concentration. In this paper, we present a simple theory that not only uses the two-state approach and reduces to MO theory in the limit of a single infinite chain, but also allows calculation of the net charge density at conditions appropriate to experiments, namely, finite chains at nonzero concentration. Our main motivation has been to establish trends as a function of concentration, chain length, and solvent quality that can be used as a guideline for experiments.

One might ask: why use a two-state model when the Poisso−Boltzmann equation gives the entire spatial distribution of counterions? The reason is that the Poisson−Boltzmann equation cannot be solved for an isotropic distribution of finite-length charged rods. It can only be solved numerically for a *fixed* configuration of rods. Thus, the PB equation is generally applied to very simple models, such as an infinitely-long rod confined in a cylindrical cell as an approximation to a periodic lattice of parallel infinite rods.[3] There are many differences between the cell model and an isotropic distribution of finite-length rods. Perhaps the most important difference is the behavior at zero concentration: the cell model yields the amount of counterion condensation predicted by Manning/Oosawa theory in the zero concentration limit, whereas a solution of finite-length rods exhibits no counterion condensation at zero concentration. To understand the concentration dependence of counterion condensation, it is therefore essential to treat a solution of finite-length rods. This is why we have adopted the more primitive two-state model.

Our approach is to use Debye−Hückel (DH) theory, extended to particles of arbitrary structure by the random phase approximation (RPA).[10−13] Debye−Hückel theory alone does not allow for nonlinear effects such as counterion condensation. This is why we augment DH theory with the two-state model, which treats the strong interactions that lead to counterion condensation by allowing for a new species, condensed counterions, which is in chemical equilibrium with free counterions. Thus, the two-state model recovers these strong interactions in the same spirit as Bjerrum pairs used in the case of electrolyte solutions.[14] The distinction between free and condensed counterions becomes less obvious at nonzero concentrations and breaks down altogether at high concentrations. However, the two-state model should be useful up to concentrations where the mesh size of the solution is comparable to the screening length due to the thickness of the condensed counterion layer. This thickness cannot be calculated within our approach, but a useful definition might be the distance at which the interaction of the counterion with a charge on a rod is of order kT; this corresponds to the Bjerrum length. There is also a lower concentration limit, because the generalized DH theory, unlike DH theory for point ions, is not exact at low densities. This is because a single polyion interacts strongly with itself, whereas the RPA assumes small deviations in the local electrostatic energy compared to kT. All of our results are therefore restricted to the semidilute regime, where both the RPA and the two-state model are useful

10.1021/ma9811021 CCC: $18.00
Published on Web 04/30/1999

approximations. It should be noted that the RPA fails to describe some features of polyelectrolyte solutions correctly, even in the semidilute regime. For example, it predicts that there is a peak in the monomer concentration structure factor, $S(k)$, that scales as $k_{max} \approx \phi_m^{1/3}$, where ϕ_m is the monomer volume fraction. Experimentally, it is known that the correct scaling is $k_{max} \approx \phi_m^{1/2}$ in the semidilute regime.[15] This defect shows that the RPA does not correctly account for interchain screening.[16] However, we have found[17] that the RPA yields a value of k_{max} that is in good *quantitative* agreement with molecular dynamics simulations of *flexible* polyelectrolytes,[18] even though the scaling is incorrect. This is possible because the semidilute regime is not very large for the chain lengths used in the simulation, so the difference in the scaling is not too apparent. We have also found that the RPA yields results for the end−end distance that are in quantitative agreement with the simulations;[13] in fact, the RPA does as well for the end−end distance as more elaborate integral equation methods that capture the correct scaling of k_{max}.[19] This suggests that the RPA provides a reasonably accurate quantitative description of no-salt polyelectrolyte solutions, at least for fairly short chains. In further support of the RPA, we note that for finite-length rods it yields the correct result of no counterion condensation at zero concentration, in contrast to recent work by Levin and Barbosa.[20] Since it predicts the correct dilute limit and is expected to be more accurate at semidilute concentrations, it should work fairly well in between. Finally, we note that we have considered only the case of no added salt; salt only affects counterion condensation significantly when the ionic strength of salt is comparable to the ionic strength of condensed counterions near the rod.

Because we have assumed an isotropic distribution of rod orientations, our results are also limited to concentrations below the isotropic/nematic transition for rods. We have estimated the transition concentration, assuming that the effective diameter of the rods can be approximated by the screening length due to free counterions and using Onsager's criterion for hard rods.[21] In all cases, the isotropic/nematic transition is far above the concentration range shown in the figures, so we are well inside the isotropic phase, as assumed.

A similar approach has been adopted by Gonzalez-Mozuelos and Olvera de la Cruz.[22] The main difference is that they use simple Debye screening by free counterions, instead of generalized Debye screening that depends on the structure of the chain. Our trends as a function of polyelectrolyte concentration, shape, and counterion valency are qualitatively consistent with theirs, but we generally find less condensation because the screening contribution from rods tends to lessen the attraction of counterions to the rods.

Finally, we remark that earlier studies of the structure of rod polyelectrolyte solutions by Canessa et al.[23] and Shew and Yethiraj[24] are quite different from ours since they did not allow for counterion condensation. They assumed a screened Coulomb interaction between charge sites on the rods, with a screening length given by the total concentration of counterions. Their approaches to the solution structure are, however, more sophisticated than our RPA treatment.

In section 2, we define the model and approach and describe the resulting free energy. In section 3, we present our results for nonzero concentrations of rigid rods of finite length in the absence of added salt. We also examine the effect of solvent quality and the resulting phase behavior of these solutions.

2. The Model

Our calculations consider an isotropic solution of n_p rigid-rod polyions in a volume V with N uniformly charged anionic monomers per rod. The bare charge for each monomer is f_o. The counterions in the solution are divided into n_f free counterions of valency z and n_c condensed counterions. Thus, the number of monomers is $n_m = Nn_p$, and charge neutrality imposes the condition $f_o n_m = zn_f + zn_c$. The monomers and counterions are all assumed to have size a. Free counterions are allowed to roam throughout the volume V, but condensed counterions are restricted to lie on the rods and reduce the local monomer charge. The condensed and free counterions are in chemical equilibrium, and so, the local monomer charge fluctuates and we consider the average number of condensed counterions per monomer $\langle\vartheta\rangle$. The net charge per monomer is then given by

$$f = f_o - z\langle\vartheta\rangle \tag{1}$$

This model is a generalization to nonzero concentration of the model introduced by Oosawa[5] to describe counterion condensation on a single infinite rod.

Our strategy is to use the random phase approximation to calculate the free energy. We then minimize it with respect to $\langle\vartheta\rangle$: this is the condition of chemical equilibrium. In this way, we can study counterion condensation as a function of the polyion concentration, length, and shape and the solvent quality. The same strategy has been applied to a single infinite rod and yields exactly the Manning/Oosawa result.[25]

Given the three species (free and condensed counterions and monomers on polyions) we can construct the local number densities of these species in solution:

$$\hat{\rho}_m(\vec{r}) = \sum_i^n \int_0^N ds\, \delta[\vec{r} - \vec{r}_i(s)]$$

$$\hat{\rho}_f(\vec{r}) = \sum_i^n \delta(\vec{r} - \vec{r}_i)$$

$$\hat{\rho}_c(\vec{r}) = \sum_i^n \int_0^N ds\, \vartheta_i(s)\, \delta[\vec{r} - \vec{r}_i(s)] \tag{2}$$

where n is the total number of chains, and $\vartheta_i(s) = 0$ if there is no condensed counterion on monomer s of chain i and 1 if there is a condensed counterion on monomer s of chain i. The charges in the system interact via electrostatic interactions, given by the Hamiltonian

$$\beta H_{el} = \frac{1}{2} l_B \int d\vec{r}\,' \int d\vec{r}\,' \frac{\hat{\rho}(\vec{r})\hat{\rho}(\vec{r}\,')}{|\vec{r} - \vec{r}\,'|} \tag{3}$$

Here l_B, the Bjerrum length, is the distance at which electrostatic interactions are equal to thermal energy, $e_0^2/\epsilon k_B T$, where e_0 is the unit charge, ϵ is the solvent dielectric constant, k_B is Boltzmann's constant, and T is the temperature. The total charge density is $\hat{\rho}(\vec{r}) = z\hat{\rho}_f(\vec{r}) + z\hat{\rho}_c(\vec{r}) - f\hat{\rho}_m(\vec{r})$. In the remainder of the paper, we will use the dimensionless Bjerrum length, $\lambda = l_B/a$, namely, the ratio of the Bjerrum length to the monomer size.

Synthetic polyelectrolytes commonly used in experiments are based on a polyvinylic backbone that can be significantly hydrophobic. For strongly as well as weakly charged polyelectrolyte solutions, the solvent quality can considerably alter the solution properties.[26,27] To incorporate the effect of the solvent quality, we include contact interactions between the monomers and the solvent:[28]

$$\beta H_{\mathrm{sol}} = {}^{v}/_{2} \int \mathrm{d}\vec{r} \int \mathrm{d}\vec{r}\,' \hat{\rho}_{\mathrm{m}}(\vec{r}) \hat{\rho}_{\mathrm{m}}(\vec{r}\,') \delta(\vec{r} - \vec{r}\,') \quad (4)$$

where v is a dimensionless excluded-volume parameter related to the Flory χ parameter by $v = 1 - 2\chi$.[29] The solvent is poor for the polyion backbone when v is negative.

To correlate the monomers into rods, we introduce a Hamiltonian βH_0 that describes the connectivity of the neutral rigid rod. This is zero if the position $\vec{r}$ is on the rod and infinite if it is not. Finally, we allow for a "binding energy" Δ of the counterion to the rod; this is the nonelectrostatic contribution to the interaction energy of a condensed counterion with a rod. In other words, this is the total interaction energy of a counterion with a monomer minus the contribution due to the Coulomb interaction between the counterion and the monomer charge.

Given these interactions, it is straightforward to construct the partition function. Although the number of polyions and counterions is fixed, the number of condensed counterions per monomer, $\langle\vartheta\rangle$, can vary.

$$\Xi = \sum_{\langle\vartheta\rangle} e^{-\Delta\langle\vartheta\rangle} Z(\langle\vartheta\rangle) \quad (5)$$

The quantity $Z(\langle\vartheta\rangle)$ is the partition function for a fixed number of condensed counterions per monomer, $\langle\vartheta\rangle$:

$$Z(\langle \mathrm{J} \rangle) = \frac{1}{n_{\mathrm{f}}! n_{\mathrm{p}}!} \frac{n_{\mathrm{m}}^{n}}{n_{\mathrm{c}}!} \int D\vec{r}_{\mathrm{m}} \int D\vec{r}_{\mathrm{f}} \int_{\text{fixed } \langle\vartheta\rangle} D\vartheta_{n}(s) \times \exp[-\beta[H_{\mathrm{o}}(\hat{\rho}_{\mathrm{m}}) + H_{\mathrm{el}}(\hat{\rho}_{\mathrm{m}}, \hat{\rho}_{\mathrm{f}}, \hat{\rho}_{\mathrm{c}}) + H_{\mathrm{sol}}(\hat{\rho}_{\mathrm{m}})]] \quad (6)$$

To carry out the integrals in eq 6, we apply the random phase approximation. This procedure assumes that the deviations from the average interactions are weak compared to thermal fluctuations (see remarks in the Introduction regarding the validity of this approximation). The fluctuations are then treated at the Gaussian level. When applied to point particle electrolytes, the RPA is equivalent to the Debye−Hückel limiting law.[30] For our system, the RPA yields the following free energy density:

$$\frac{\beta\Omega}{V} = \frac{\phi_{\mathrm{m}}}{N} \log \phi_{\mathrm{m}} + \phi_{\mathrm{f}} \log \phi_{\mathrm{f}} + \langle\vartheta\rangle \phi_{\mathrm{m}} \log \langle\vartheta\rangle - \frac{1}{2} v \phi_{\mathrm{m}}^{2} + \frac{1}{6} \phi_{\mathrm{m}}^{3} + \frac{\Delta\langle\vartheta\rangle}{V} + \frac{1}{2} \frac{1}{(2\pi)^{3}} \int \mathrm{d}\vec{k} \times \log\left[1 + \frac{\kappa^{2}(\vec{k})}{k^{2}} + v \phi_{\mathrm{m}} N\, g(\vec{k}) \frac{4\pi\lambda\phi_{\mathrm{f}}}{k^{2}}\right] \quad (7)$$

The first three terms in eq 7 contain the contributions from entropy of mixing of the polyions, free counterions, and condensed counterions, respectively. The free counterions explore the entire volume V, but the condensed counterions are constrained to lie on the rods so their entropy is reduced. Here, ϕ_{m}, ϕ_{f}, and ϕ_{c} are the volume fractions of monomers, free counterions, and condensed counterions, respectively. The fourth and fifth terms are the standard second and third virial terms for a polymer in solution. The last term represents the *screened* electrostatic interaction energy arising from one-loop corrections to the neutral system. The wavevector-dependent inverse screening length $\kappa(\vec{k})$ depends on the structure of the interacting particles.[11−13] When all species are taken to be point particles, $\kappa^2(k)$ reduces to $\kappa^2 = 4\pi\lambda(f^2\phi_{\mathrm{m}} + z^2\phi_{\mathrm{f}})$, and the last term in eq 7 reduces to $-\kappa^3/12\pi$ once the self-energy is subtracted. This is the well-known Debye−Hückel result. When we take the polyions to be rigid rods and assume all other species to be point particles, we have

$$\kappa^{2}(\vec{k}) = 4\pi\lambda[f^{2}\phi_{\mathrm{m}} N\, g(k) + z^{2}\phi_{\mathrm{f}}] \quad (8)$$

where $g(k) = N/k \int_{-kN}^{kN} \mathrm{d}x(1 - \cos x)/x^2$ is the isotropic rigid-rod form factor. Since $g(k)$ vanishes for large wavevectors k, only the free counterions screen at short distances of interaction. For small wavevectors corresponding to long interaction distances, both the free counterions and the polyions contribute to screening. Note that the screening contribution made by the polyions is proportional to the *net* charge f on the polyion. The third term inside the integral in eq 7, $v\phi_{\mathrm{m}} N g(k) 4\pi\lambda\phi_{\mathrm{f}}/k^2$, describes the coupling between the van der Waals and electrostatic interactions at the one-loop level. Note that the entropy of mixing favors *fewer* condensed counterions, but the interaction energy favors *more* condensed counterions.

As written, the integral over $\vec{k}$ in eq 7 includes the self-energy and the energy of a monomer or a free counterion electrostatically interacting with itself at distances smaller than $2a$. To avoid counting these redundant interactions in the free energy, the self-energy is often subtracted from the full integral.[6,31,32] Rather than subtract a polyion structure-dependent quantity,[33] we apply an upper wavevector cutoff to the integral. Allowing the maximum wavevector $|k|$ to be $\Lambda = \pi/a$ corresponds to prohibiting ions from interacting at distances closer than the diameter of the molecules. This is the only way in which we take into account the nonzero diameter of the rods and counterions, and it eliminates the self-energy from the integral altogether. For convenience, we take the nonelectrostatic binding energy Δ to be zero. Note, however, that the effect of a positive value of Δ is to increase the amount of condensation since there are other interactions beyond the Coulomb interaction that attract the counterion to the rod.

3. Results

A. θ Solvent. To determine the average number of condensed counterions per monomer and thus the net charge per monomer at equilibrium, we minimize the free energy in eq 7 with respect to $\langle\vartheta\rangle$. We consider first the case of θ solvent and examine trends in polyion concentration, chain length, chain shape, and counterion valency.

The effect of polyion concentration on counterion condensation is shown in Figure 1 where we compare the average net charge per monomer f for a series of polyion concentrations. The solid curve corresponds to the MO result for a single, infinitely long rod. According to MO theory, all counterions are free at low charge densities or high temperatures where entropy of mixing

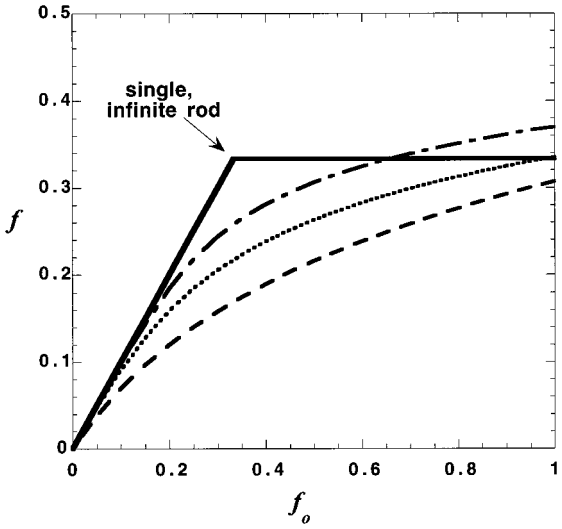

Figure 1. Effect of polyion concentration on counterion condensation. The reduced net charge per monomer f vs the bare-rod charge per monomer f_0 for three monomer volume fractions ϕ_m of isotropic solutions of finite rods ($\phi_m = 0.01$, dashed; $\phi_m = 0.001$, dotted; and $\phi_m = 0.0001$, dot−dashed). The solid line is the MO result for a single, infinite rod. The parameters used here ($\lambda = 3$, $N = 30$, and $z = 1$) are appropriate to describe polystyrene sulfonate at room temperature in water: $\phi_m = 0.01$ corresponds to a 0.3 monomolar solution. The overlap concentration for these rods is near $\phi_m = 0.001$.

dominates, namely, where $\lambda f_o < 1$, for monovalent counterions. Thus, for $\lambda f_o < 1$, the net charge density is equal to the bare charge density ($f = f_o$). For $\lambda f_o > 1$, the electrostatics are strong enough to draw some counterions near the rod, and thus, the net charge is reduced. As the bare charge increases or, equivalently, as the temperature decreases, the net charge saturates such that the rod maintains 1 counterion per Bjerrum length. We find that as the polyion concentration increases the net charge significantly decreases; i.e., more counterion condensation occurs with increased polyion concentration. Evidently, the dominant effect is an entropic one: as the solution becomes more crowded, the entropic penalty for condensed counterions is reduced. The bare charge can be varied experimentally, for example, by synthesizing chains with different fractions of charged monomers in a copolymer of charged and uncharged groups.[26] In the case of a polyacid or polybase, f_o can be changed by adjusting the pH.

Figure 1 also shows that the onset of counterion condensation occurs well below $\lambda f_o = 1$ at nonzero concentrations, demonstrating that counterion condensation becomes significant at much lower charge fractions or, equivalently, much higher temperatures than those predicted by MO for zero concentration.

It is interesting to note that the net charge at nonzero concentrations does not saturate to one charge per Bjerrum length as it does in the single, infinite rod case. However, X-ray and neutron scattering experiments on solutions of *flexible* polyelectrolytes show a saturation in the net charge.[7,27] Our results for rigid polyions suggest that the saturation is not due to effects contained in MO theory and that the physical explanation of the saturation remains to be elucidated for flexible chains.

We note that the observation of increased counterion condensation with concentration is not new; it has been clearly shown with lattice theories that condensation

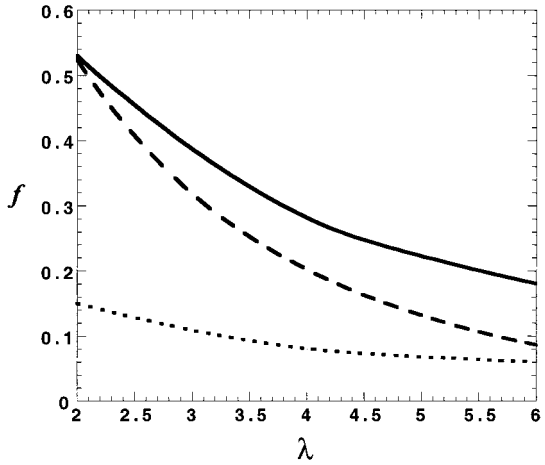

Figure 2. Comparison of our results to the theory of Gonzalez-Mozuelos and Olvera de la Cruz. The average net charge per monomer f is compared over a range of temperatures λ for monovalent counterions at a monomer concentration $\phi_m = 0.0027$, with $N = 3000$. The solid curve corresponds to the MO result for a single, infinitely long rod. Our results (dashed curve) show considerably less counterion condensation than theirs (dotted curve) because of the screening of the rods.

is enhanced at higher concentration.[34−36] However, these approaches treat either spheres or infinitely long chains placed in a periodic array, whereas ours treats finite-length chains placed at random. A similar trend was also observed by Gonzalez-Mozuelos and Olvera de la Cruz for finite chains at nonzero concentration, using a different approach. However, we find considerably less counterion condensation than they do. A direct comparison of our results to those of Figure 4 of Gonzalez-Mozuelos and Olvera de la Cruz[22] is shown in Figure 2. Here, we compare the average net charge per monomer f for a series of polyion concentrations. The solid curve corresponds to the MO result for a single, infinitely long rod. Our results (dashed curve) show much less condensation than theirs (dotted curve). The difference arises from the way we treat electrostatic screening. In their case, only the free counterions screen electrostatic interactions. In our case, the rods also contribute to screening; this is why our screening parameter depends on wavevector. Since there is more screening in our case, the electrostatic attraction of counterions to the rods is weaker, so there is less counterion condensation.

A single macroion of finite size at zero concentration does not undergo counterion condensation because the entropic gain of the free macroions is always greater than the electrostatic attraction to the macroion. However, even quite dilute solutions of short rods show a reduction in net charge compared to the single, infinite rod at zero concentration. Figure 3 compares the results for different rod lengths. For a counterion interacting at a distance r from a rod of length L, the electrostatic potential ψ behaves as an infinite rod at small $r \ll L$; i.e., it varies as $-\log r$. At large $r > L$, the electrostatic potential varies as $1/r$, as for a point particle. The longer the rod, the larger the r at which the crossover occurs between infinite-rod and point-particle behavior. As shown in Figure 3, more counterion condensation takes place in solutions of longer rods.

The dependence of our interaction energy on polyion structure enables us to test the importance of polyion shape on counterion condensation. In a comparison of rigid spherical polyions to rigid-rod polyions, we show that shape has a significant effect on counterion con-

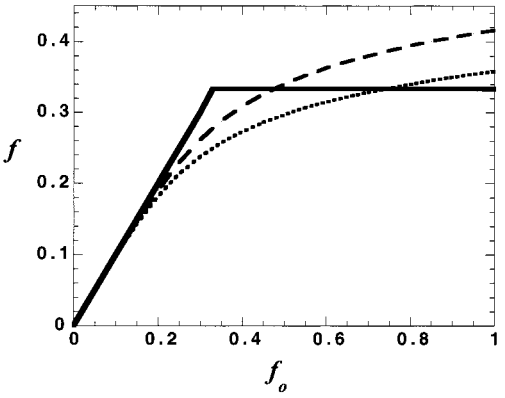

Figure 3. Effect of finite rod length on counterion condensation. Dilute solutions of short rods ($N = 10$, dashed, and $N = 100$, dotted) do undergo some counterion condensation. Longer rods attract counterions more strongly. Here, $\lambda = 3$ and $\phi_m = 10^{-4}$.

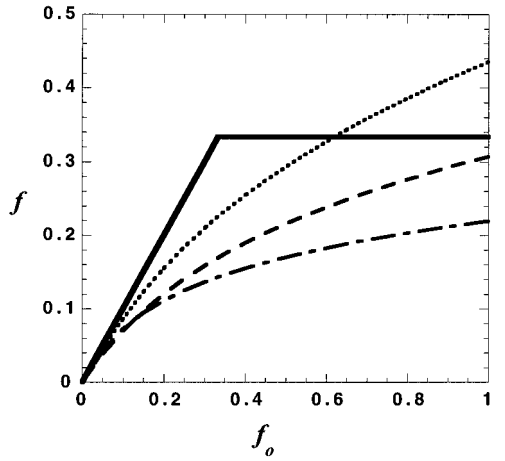

Figure 4. Effect of rigid shape on counterion condensation. The dashed curve shows the net charge for a solution of 30 monomer long rods. The dotted curve shows the net charge for a solution of spheres with 30 monomer diameters. Solutions of rigid rods display more counterion condensation than solutions of comparably sized spheres. The dot−dashed curve shows the net charge for a solution of spheres with 12 monomer diameters. These spheres are more compact than the rods but have the same bare charge. Because of the higher charge density in these smaller spheres, this solution undergoes more counterion condensation than the solution of rods ($\lambda = 3$, $\phi_m = 0.01$, and $N = 30$).

densation (Figure 4). A solution of rods of length N undergoes more counterion condensation (dashed curve) than a solution of spheres of the same total bare charge with diameter N (dotted curve). However, for solutions of smaller spheres carrying the same total bare charge (dot−dashed curve), more counterion condensation occurs than for the rod solution because of the higher charge density on the compacted spheres, which enables them to attract counterions more strongly. This trend is consistent with an alternate theory by Gonzalez-Mozuelos and Olvera de la Cruz.[22] Given that a flexible chain takes on an equilibrium conformation that lies between the extended rod shape and the tightly compacted sphere, we expect flexibility of the polyion structure to play a key role in the amount of counterion condensation occurring in experiments. In addition, because the chain structure depends strongly on the interactions with surrounding counterions, the interplay between chain structure and counterion condensation is likely to be very rich. Simulations by Stevens and

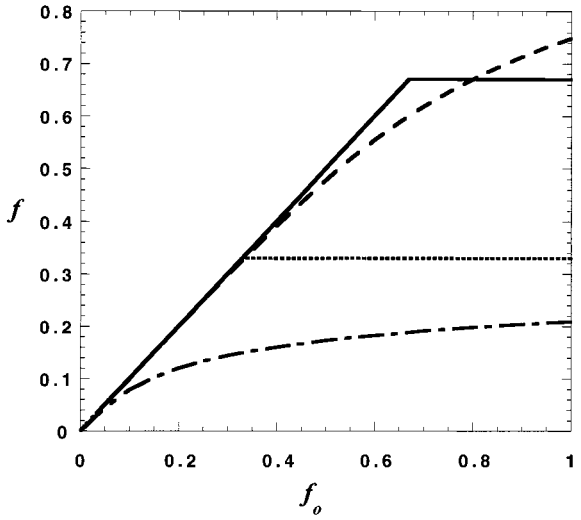

Figure 5. Comparison of monovalent and divalent counterions. The solid curve shows the MO result for the monovalent case. The dashed curve represents our results for monovalent counterions. The dotted curve represents the MO divalent case, and the dot−dashed curve shows our divalent counterion results ($\lambda = 1.5$, $\phi_m = 0.0001$, and $N = 30$).

Kremer[18] show that counterions can mediate intrachain attractions that substantially alter the structure of flexible polyelectrolytes. Recent theoretical work by Gonzalez-Mozuelos and Olvera de la Cruz also predicts this trend.[22]

We have also examined the effect of counterion valency on condensation. More counterion condensation is expected with multivalent counterions than with monovalent counterions, even in the infinitely dilute limit of MO theory. However, as Figure 5 shows, the effect of valence is even stronger at nonzero concentrations. Here we have plotted the MO results for monovalent (solid curve) and divalent (dotted curve) counterions. In addition, we have plotted our results at a concentration of $\psi_m = 10^{-4}$ for monovalent (dashed) and divalent (dot−dashed) counterions. Note that for divalent counterions the amount of counterion condensation does appear to saturate at higher f, in better qualitative (although not quantitative) agreement with MO theory.

For monovalent counterions, the theory of Gonzalez-Mozuelos and Olvera de la Cruz[22] predicts significantly more counterion condensation than our theory does, as already shown in Figure 2. However, for divalent counterions, the results are more comparable. The main difference between the theories is that we have included the contribution of rods to electrostatic screening. As the counterion valency increases, the contribution of rods to screening becomes less important relative to the contribution of counterions, so our results converge with theirs for multivalent counterions.

Counterion condensation has a strong effect on the osmotic pressure of a polyelectrolyte solution. The osmotic pressure is given by

$$\beta\Pi = \frac{\partial \log Z(\langle\vartheta\rangle)}{\vartheta V}\Big|_{N,T} \tag{9}$$

To study the amount of counterion condensation, we examine the ratio of the osmotic pressure to the osmotic pressure if all of the counterions were free and were treated as an ideal gas (Π_{ideal}). This ratio is called the osmotic coefficient. At zero concentration, the osmotic

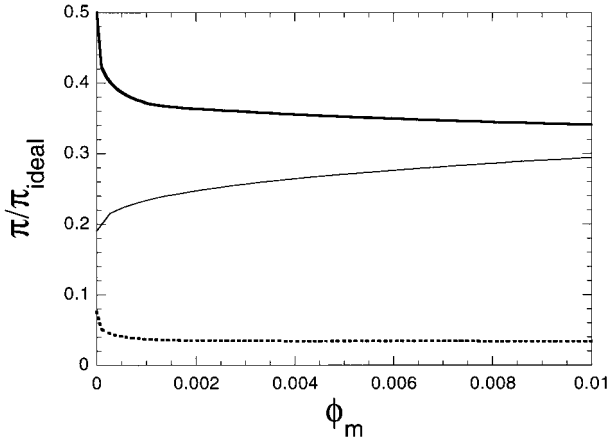

Figure 6. Osmotic coefficient (ratio of osmotic pressure to osmotic pressure of ideal gas of counterions, Π/Π_{ideal}) as a function of monomer concentration ϕ_m in θ solvent. Our results for monovalent (thick solid) and divalent (dashed) counterions show that the osmotic coefficient decreases with increasing concentration (more condensation). In contrast, we show the results of the exact solution of the Poisson−Boltzmann equation for an infinite line charge in a cylindrical cell whose diameter is determined by the concentration ϕ_m. The behavior is qualitatively different, because the cell model yields counterion condensation at zero concentration ($\lambda = 3$, $N = 30$, and $f_0 = 1$).

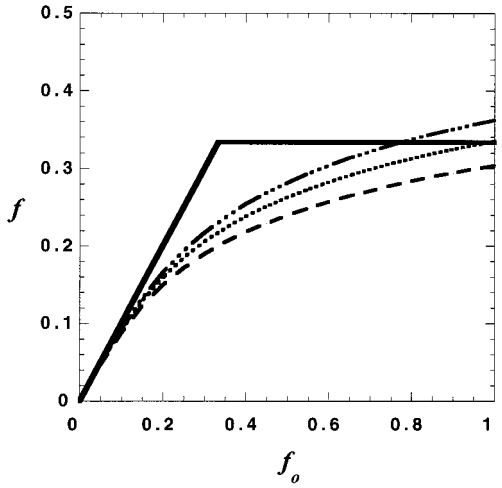

Figure 7. Effect of solvent quality on counterion condensation. The net charge vs. bare charge curves for poor solvent ($v = -20$, dashed), θ solvent ($v = 0$, dotted), and good solvent ($v = 20$, dot−dashed). The net charge decreases as the solvent becomes poorer ($\lambda = 3$, $\phi_m = 0.001$, and $N = 30$).

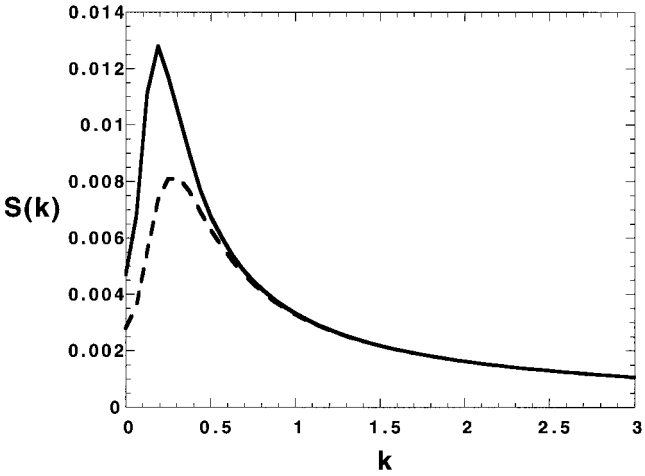

Figure 8. Predicted monomer−monomer structure factor when counterion condensation is taken into account (solid) and when it is assumed not to occur (dashed). The solution is in poor solvent with $\lambda = 3$, $\phi_m = 0.001$, $N = 30$, and $f_0 = 1$.

coefficient Π/Π_{ideal} is unity, because there is no counterion condensation. Figure 6 shows that the ratio rapidly drops to a value smaller than unity as the monomer concentration increases (thick solid curve). For comparison, we have also shown the result based on the exact solution to the Poisson−Boltzmann equation within the cell model (thin solid curve).[37] The concentration dependence of the cell model result is completely different, because the cell model for infinite rods predicts that there is counterion condensation even at zero concentration. In fact, the cell model (incorrectly) predicts that the ratio Π/Π_{ideal} should *increase* rather than decrease with increasing concentration. Thus, this figure demonstrates the utility of our approach as compared to the cell model. In Figure 6, we have also shown our results for divalent counterions (dashed curve) to show that there is far more condensation for divalent than monovalent counterions, as expected.

B. Poor Solvent and Phase Behavior. In poor solvent, there is an attractive interaction between polymer chains. This attraction competes with electrostatic repulsion, but it should lead to larger concentration fluctuations than in the θ solvent case treated above. Because counterion condensation depends sensitively on concentration, we might expect solvent quality to affect condensation. Here, we imagine tuning the solvent quality by changing the solvent without changing the electrostatic interactions, i.e., a fixed solvent dielectric constant. The resulting effect of solvent quality on counterion condensation is shown in Figure 7. The net charge is lower in poor solvent than in good solvent. As the solvent quality decreases, there is more counterion condensation.

When we tune the solvent quality v at fixed bare charge f_o, the effect on counterion condensation leads to interesting phase behavior. Because the solvent is poor, the system prefers to phase separate into polymer-rich and polymer-poor phases. However, charge neutrality dictates that the counterions must accompany the polyions in the condensed phase, resulting in a very large entropy cost. In the absence of counterion condensation, Borue and Erukimovich[11] and Joanny and Leibler[12], have shown that solutions can undergo *meso*phase separation into chain-rich and chain-poor domains that locally violate charge neutrality so that counterions need not relinquish their entropy to join the chain-rich domains. The signature of the mesophase transition is the divergence of the peak of the monomer−monomer structure factor in solution $S(k)$ occurring at nonzero wavevector k. Within the RPA, the monomer−monomer structure factor in solution is given by[12]

$$S(k) = \frac{4\pi\lambda z^2\phi_f + k^2}{(4\pi\lambda z^2\phi_f)\,([\phi_m N\, g(k)]^{-1} + v) + 4\pi\lambda f^2} \quad (10)$$

Figure 8 shows the peak in $S(k)$ in poor solvent at a fixed bare charge with and without counterion condensation. When counterion condensation is taken into consideration, the reduced net charge on the polyion leads to $S(k)$ divergence at a *lower* wavevector k than that of the same system of rods without counterion condensation. We now tune the solvent quality at fixed

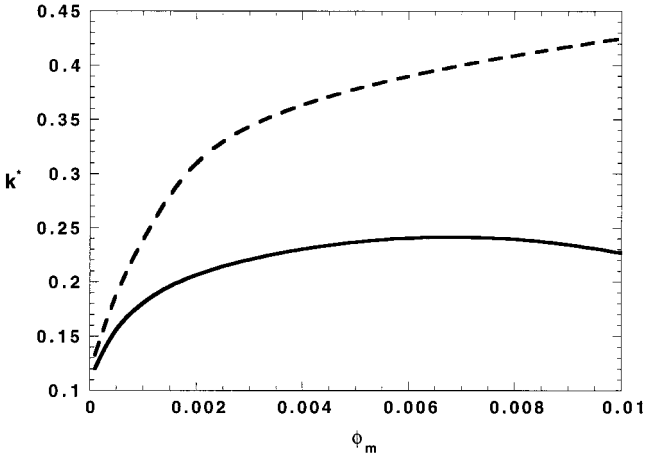

Figure 9. Mesophase separation when counterion condensation is taken into account (solid) and when it is not (dashed). The wavevector k^* leads to a divergence in the monomer−monomer structure factor peak vs. polyion concentration. The mesophase domain size is related to k_c as $2\pi/k_c$. Thus, the predicted domain size is much larger when counterion condensation is taken into account. Parameters used here are $\lambda = 3$, $\phi_m = 0.001$, $N = 30$, and $f_0 = 1$.

bare charge and examine the *divergence* of the peak in $S(\vec{k})$, where the transition takes place. Figure 9 compares the wavevector $\vec{k}^*$ of the peak divergence versus polyion concentration for solutions when counterion condensation is allowed and when it is assumed not to occur. The characteristic domain size of the mesophases is inversely related to $\vec{k}^*$. Hence, when counterion condensation is considered, considerably larger domains are formed. When we compare the critical solvent quality, the value of v at which $S(\vec{k})$ diverges for a given f, the mesophase transition takes place in better solvent than predicted in the absence of condensation. For example, at a volume fraction of $\phi_m = 0.001$ for rods of length $N = 10$ at a temperature $\lambda = 3$ and charge fraction $f_0 = 1$, the critical solvent quality v^* is 40% higher with counterion condensation than without. Physically, condensed counterions relinquish less entropy than free counterions in joining the mesophase. Therefore, when counterion condensation is included, the monomer−solvent repulsion need not be as strong to overcome the counterion entropy of mixing.

4. Discussion

Recently, it has been shown that condensed counterion fluctuations along the lengths of the rods lead to short-ranged attractive interactions between rods that effectively reduce the solvent quality.[38,25,39] For multivalent counterions, these attractions are sufficiently strong to overwhelm the electrostatic repulsion between like-charged chains. Because we have assumed that the condensed counterions are distributed uniformly along the chains, we have neglected these effects here. This counterion-mediated attraction can give rise to interesting phase behavior[39] and could certainly have a strong impact on thermodynamic solution properties.

In systems of flexible polyelectrolytes, counterion-mediated attractions can have even stronger effects.[22,6] Stevens and Kremer[18] have shown numerically that these attractions cause contraction of chains. Our results indicate that contraction could lead to further condensation, which could lead to a stronger attraction, and so on. These effects might explain the saturation of the net charge that is observed experimentally.[7,27] The generalization of our approach to flexible chains should shed light on this issue.

Acknowledgment. We thank James P. Donley, Ludwik Leibler, and Claudine Williams for instructive discussions. The support of the National Institutes of Health through Grant 5T3 GM08496-04 (R.M.N.) and the National Science Foundation through Grant DMR-9619277 (B.Y.H. and A.J.L.) are gratefully acknowledged.

References and Notes

(1) LeBret, M.; Zimm, B. *Biopolymers* **1984**, *23*, 287.
(2) Fixman, *M. J. Chem. Phys.* **1979**, *70*, 4995.
(3) Fuoss, M.; Katchalsky, A.; Lifson, S. *Proc. Natl. Acad. Sci.* (U.S.A.) **1951**, *37*, 579.
(4) Manning, G. S. *J. Chem. Phys.* **1969**, *51*, 954.
(5) Oosawa, F. *Polyelectrolytes*; Marcel Dekker: New York, 1971.
(6) Olvera de la Cruz, M.; Belloni, L.; Delsanti, M.; Dalbiez, J. P.; Spalla, O.; Drifford, M. *J. Chem. Phys.* **1995**, *103*, 5781.
(7) Essafi, W.; Lafuma, F.; Williams, C. E. *Macromolecules*, submitted for publication.
(8) Ermi, B. D.; Amis, E. J. *Macromolecules* **1996**, *29*, 2701.
(9) Gao, J. Y.; Dubin, P. L.; Sato, T.; Morishima, Y. *J. Chromotogr. A* **1997**, *766*, 233.
(10) Khokhlov, A. R.; Khachaturian, K. A. *Polymer* **1982**, *23*, 1742.
(11) Borue, V. Yu.; Erukimovich, I. Ya. *Macromolecules* **1988**, *21*, 3240.
(12) Joanny, J.-F.; Leibler, L. *J. Phys. (Paris)* **1990**, *51*, 545.
(13) Donley, J. P.; Rudnick, J.; Liu, A. J. *Macromolecules* **1996**, *4*, 1188.
(14) Fisher, M. E.; Levin, Y. *Physica A* **1996**, *225*, 164.
(15) Drifford, M.; Dalbiez, J.-P. *J. Phys. Chem.* **1984**, *88*, 5368.
(16) Donley, J. P.; Rajasekaran, J. J.; Liu, A. J. *J. Chem. Phys.*, in press.
(17) Donley, J. P.; Liu, A. J. Unpublished results.
(18) Stevens, M.; Kremer, K. *J. Chem. Phys.* **1995**, *103*, 1669.
(19) Yethiraj, A. *J. Chem. Phys.* **1998**, *108*, 1184; *Phys. Rev. Lett.* **1997**, *78*, 3789.
(20) Levin, Y.; Barbosa, M. C. *J. Phys. II (Paris)* **1997**, *7*, 37.
(21) Onsager, L. *Ann. N. Y. Acad. Sci.* **1949**, *15*, 627.
(22) Gonzalez-Mozuelos, P.; Olvera de la Cruz, M. *J. Chem. Phys.* **1995**, *103*, 3145.
(23) Canessa, E.; Daguanno, B.; Weyerich, B.; Klein, R. *Mol. Phys.* **1991**, *73*, 175. Weyerich, B.; Daguanno, B.; Canessa, E.; Klein, R. *Faraday Discuss. Chem. Soc.*, **1990**, *90*, 245.
(24) Shew, C. Y.; Yethiraj, A. *J. Chem. Phys.* **1997**, *106*, 5706. Yethiraj, A.; Shew, C. Y. *Phys. Rev. Lett.* **1996**, *77*, 3937.
(25) Ha, B.-Y.; Liu, A. J. *Phys. Rev. Lett.* **1997**, *79* (7), 1289.
(26) Essafi, W.; Lafuma, F.; Williams, C. E. *J. Phys. II (Paris)* **1995**, *5*, 1269.
(27) Ermi, B. D.; Amis, E. J. *Macromolecules* **1997**, *30*, 6937.
(28) Doi, M.; Edwards, S. F. *The Theory of Polymer Dynamics*; Oxford University Press, New York, 1986.
(29) deGennes, P.-G. *Scaling Concepts in Polymer Physics*: Cornell University Press, 1979.
(30) Brout, R., Caruthers, P. *Lectures on the Many Electron Problem*; Interscience: New York, 1963; Chapter 1.
(31) Warren, P. *J. Phys. II (Paris)* **1997**, *7*, 343.
(32) Anderson, H. C.; Chandler, D. *J. Chem. Phys.* **1971**, *55*, 1497.
(33) The appropriate self-energy for our system is

$$-\int \mathrm{d}\vec{k}(4\pi\lambda/k^2)(f^2\phi_m N\, g(\vec{k}) + z^2\phi_f)$$

(34) Alexander, S.; Chaikin, P. M.; Grant, P.; Morales, G. J.; Pincus, P. *J. Chem. Phys.* **1984**, *80*, 5776.
(35) Ramanathan, G. V.; Woodbury, C. P. *J. Chem. Phys.* **1985**, *82*, 1482.
(36) Stevens, M. J.; Falk, M. L.; Robbins, M. O. *J. Chem. Phys.* **1996**, *104*, 5209.
(37) Katchalsky, A. *Pure Appl. Chem.* **1971**, *26*, 327. Katchalsky, A.; Alexandrowicz, Z.; Kedem, O. In *Chemical Physics of Ionic Solutions*; Conway, B. E., Barradas, R. G., Eds.; Wiley: New York, 1966.
(38) Grønbech-Jensen, N.; Mashl, R. J.; Bruinsma, R. F.; Gelbart, W. M. *Phys. Rev. Lett.* **1997**, *78*, 2477.
(39) Ha, B.-Y.; Liu, A. J. *Phys. Rev. Lett.* **1998**, *81*, 1011.

MA9811021